



Investigations of void formation in neutron irradiated iron and F82H steel

Eldrup, Morten Mostgaard; Singh, Bachu Narain

Publication date:
2002

Document Version
Publisher's PDF, also known as Version of record

[Link back to DTU Orbit](#)

Citation (APA):
Eldrup, M. M., & Singh, B. N. (2002). *Investigations of void formation in neutron irradiated iron and F82H steel*. Risø National Laboratory. Denmark. Forskningscenter Risø. Risø-R No. 1241(EN)

General rights

Copyright and moral rights for the publications made accessible in the public portal are retained by the authors and/or other copyright owners and it is a condition of accessing publications that users recognise and abide by the legal requirements associated with these rights.

- Users may download and print one copy of any publication from the public portal for the purpose of private study or research.
- You may not further distribute the material or use it for any profit-making activity or commercial gain
- You may freely distribute the URL identifying the publication in the public portal

If you believe that this document breaches copyright please contact us providing details, and we will remove access to the work immediately and investigate your claim.

Investigations of Void Formation in Neutron Irradiated Iron and F82H Steel

M. Eldrup and B.N. Singh

**Materials Research Department
Risø National Laboratory, Roskilde
December 2001**

Abstract In the present work pure iron and low activation steel F82H have been neutron irradiated at temperatures in the interval 50°C - 350°C to a dose of 0.23 dpa (displacements per atom). The formation of defects has been investigated by the use of positron annihilation spectroscopy (PAS). In addition iron has been irradiated to different doses in the range 0.01 - 0.4 dpa at 50°C and 100°C and the dose dependence of the electrical conductivity determined.

The results demonstrated that the formation of voids takes place during neutron irradiation of pure iron in the whole temperature range. For irradiation temperatures of 50°C and 100°C also a high density of micro-voids was observed. Voids and micro-voids were also detected in low activation F82H steel for a low irradiation temperature (50°C), while for irradiation close to the temperature of annealing stage V (250°C), no voids or micro-voids could be detected. Surprisingly, irradiation at the higher temperature of 350°C again resulted in void formation. The annealing behaviour of iron irradiated at 50°C and at 100°C did not show any significant difference. Coarsening of the micro-void and void population takes place below stage V by migration and coalescence of the micro-voids and voids.

The dose dependence of the electrical conductivity of iron showed a lower conductivity for the specimens irradiated at 50°C than at 100°C. This has been associated with the segregation of carbon at about 70°C where carbon becomes mobile.

ISBN 87-550-2824-1
ISBN 87-550-2826-8 (Internet)
ISSN 0104-2840

Print: Pitney Bowes Management Services Denmark A/S, 2002

Contents

1	Introduction	5
2	Characterization of Defects and Defect Agglomerates by PAS	5
3	Materials and Experimental Procedure	6
4	Results	7
5	Discussion	8
5.1	As-irradiated Fe and F82H	8
5.2	Annealing of Fe	10
5.3	Electrical Conductivity	11
6	Summary	11
	Acknowledgement	12
	References	12

1 Introduction

Low activation steels are considered as candidate materials for the blanket and first wall of fusion reactors. Therefore extensive studies of the effects of neutron irradiation on the microstructure and the physical and mechanical properties of these materials are being carried out. The present work was initiated to take advantage of the ability of positron annihilation spectroscopy (PAS) to detect the presence of single vacancies, vacancy clusters, microscopic and sub-microscopic voids and other vacancy type defects [1]. We have used the technique to study the evolution of voids during neutron irradiation at different temperatures in pure iron and in F82H steel. Furthermore it was decided to investigate the defect evolution during post-irradiation isochronal annealing of iron specimens irradiated at 50°C for comparison with previous measurements of the annealing behaviour after irradiation at 100°C. In addition, the dose dependence of the electrical conductivity was measured for iron irradiated at 50°C and at 100°C.

In the following section (Section 2) a brief outline of the basis of defect characterization by PAS is given. This is followed by details of materials and experimental procedures used in the present investigation (Section 3). The results are described in Section 4. The physical meaning of the results and their implications regarding void nucleation are discussed in Section 5. The main conclusions are presented in Section 6.

2 Characterization of Defects and Defect Agglomerates by PAS

The physical basis for the use of positrons in defect studies is the fact that positrons injected into a material may get trapped at defects that represent regions where the atomic density is lower than the average density in the bulk, i.e. vacancies, vacancy clusters (including voids and bubbles) and dislocations. Since positrons and electrons are antiparticles, an injected positron will annihilate with an electron of the material. As a result, gamma rays will be emitted. These γ -quanta carry information about the state of the positron before annihilation, and by proper measurement of the emitted γ -quanta, it is therefore possible to obtain useful information about those defects that have trapped the positrons. This is in brief the physics behind the so-called Positron Annihilation Spectroscopy (PAS), which comprises several different experimental techniques. A more detailed discussion of PAS can be found in e.g. [1, 2] and references therein. In the present work the positron lifetime technique has been applied to measure the distribution of lifetimes of the injected positrons, a so-called positron lifetime spectrum.

Normally, regions of lower-than-average atomic density also have lower-than-average electron density. The lifetime of positrons trapped in defects will depend on the average electron density in the defects (the lower the electron density, the longer is the lifetime). So in principle, each type of defect gives rise to a characteristic positron lifetime, τ_i . In cases where several types of defects are present in a sample, a lifetime spectrum will therefore be measured that consists of several lifetime components. Each component is a decaying exponential, the slope of which equals the annihilation rate ($= \tau_i^{-1}$). One example of positron lifetime spectra is

shown in Fig. 1. The figure shows spectra for un-irradiated iron as well as iron neutron irradiated at different temperatures and displays both single- and multi-component spectra. The aim of a numerical analysis of a lifetime spectrum is to separate the various components and to determine their lifetimes τ_i and their intensities I_i . Usually, the lifetimes are numbered from the shorter to the longer lifetimes (τ_1, τ_2, τ_3 , etc.). An intensity of a component, which is defined as the relative area of that component, gives a measure of the fraction of positrons that annihilate with the equivalent lifetime. In practice, it is possible to resolve only two or three lifetime components in a spectrum for a metal, so in the data analysis, in some cases two or more components may merge into one.

In bulk Fe the positron lifetime is 106 ps, while in defects such as monovacancies, dislocations, loops and SFTs the lifetimes are found to be in the range of ~ 120 - ~ 180 ps [3 - 10]. The lifetime of positrons trapped in three-dimensional vacancy agglomerates (voids) increases with the size of the voids up to a saturation value of about 500 ps for voids containing more than ~ 40 - 50 vacancies [1, 7 - 9]. Thus, for small, sub-microscopic voids (that we shall refer to as micro-voids) the lifetime value is a measure of their size.

3 Materials and Experimental Procedure

Thin sheets of pure iron were purchased from Goodfellow (England) in cold-worked state. To obtain fully recrystallized material, the iron was annealed at 650°C for 2 hours in vacuum ($\sim 10^{-4}$ Pa). The F82H low activation steel was obtained from the common European stock available at PSI (Switzerland) in the as-tempered condition. The tempering heat treatment consisted of solution annealing at 1050 - 1075°C for 2 hours followed by air cooling and ageing at 750°C for 1 hour followed by air cooling. The steel was used in the as-tempered condition.

The specimens used for the PAS and electrical conductivity measurements were tensile test specimens [11]. The purity of the iron and the composition of the F82H steel are given in Table 1. The sample thickness was 0.25 - 0.3 mm for both materials. These specimens were neutron irradiated in the DR-3 reactor at Risø at temperatures in the range of 50°C - 350°C to a fluence of 1.5×10^{24} n/m² ($E > 1$ MeV) equivalent to ~ 0.23 displacements per atom (NRT) (dpa). For the PAS measurements, two samples of approximately 6×5 mm were cut from one tensile specimen. Before isochronal annealing and PAS measurements were carried out, the sample surfaces were cleaned by electropolishing.

The Fe specimens irradiated at 50°C were isochronally annealed in vacuum ($\sim 2 \times 10^{-4}$ Pa) in steps of 50°C with a hold time of 50 min. at each annealing step. Positron lifetime measurements were carried out after each step.

For the PAS measurements a ^{22}Na positron source (encapsulated in two thin Ni foils) was placed between the two samples that had been cut from the tensile specimen.

The radioactivity of the samples may give rise to an additional component in a measured lifetime spectrum unless special precautions are taken. As described in

[12] this can be done by using a three-detector coincidence technique, which reduces the additional component intensity to an insignificant level.

The measured lifetime spectra contained a total number of counts in the range of $1 - 3 \times 10^6$. In several cases spectra were measured more than once to ensure reproducibility. In parallel with the measurements on the irradiated Fe and F82H, reference spectra for well-annealed Cu were recorded under - as far as possible - identical experimental conditions [12].

The measured lifetime spectra were analysed with the PATFIT programs [13]. The reference spectra were used to determine the time resolution of the spectrometer and the correction for positrons annihilating in the source. Small variations of the time resolution during the measuring period were taken into account in the analysis of the spectra.

4 Results

To illustrate directly the obtained positron lifetime data for iron and F82H steel at different irradiation temperatures, the lifetime spectra are shown in Figs. 1 and 2. Clearly, the spectra for Fe and F82H are qualitatively similar, but quantitatively different. For both materials irradiation gives rise to an increase in the average positron lifetime at all irradiation temperatures, most pronounced in iron irradiated at 50°C and 100°C. These changes in lifetime are the signatures of the creation of defects during irradiation.

Quantitative analyses showed that the lifetime spectra for both Fe and F82H could be resolved into three lifetime components for all irradiation and annealing temperatures. In general, the longest lifetime, τ_3 scatters a few ps around ~ 500 ps. This lifetime is in the range expected for large 3-dimensional vacancy agglomerates, i.e. voids that contain more than 40 - 50 vacancies. In order to reduce the scatter on the other lifetimes and intensities we have therefore fixed τ_3 to its average value in the final analyses of the lifetime spectra. The three lifetimes and the intensities of the two most long-lived components as functions of irradiation temperature are shown for both Fe and F82H in Fig. 3.

Trapping of positrons into one type of defects takes place in competition with trapping into other types of defects and with annihilation in the bulk. This competition has been modelled by simple rate equations, often referred to as the "trapping model" [1]. If the trapping rates are comparable to the annihilation rate of the positrons in the bulk, the trapping model can be used to obtain quantitative estimates of these trapping rates. Trapping rates can normally to a good approximation be assumed to be proportional to the concentrations of the defects, i.e.

$$\kappa_i = \mu_i \times C_i \quad (1)$$

where κ_i is the trapping rate into the defects of type 'i' and C_i their density. Hence, if the so-called specific trapping rate μ_i is known, the defect densities can be estimated. The specific trapping rate is different for different types of defects. Theoretical estimates have been made of μ_i for various defect types and compared with values determined experimentally [14]. For voids, for example, the experimental estimate of μ_{void} demonstrates that it increases with void size [1].

The trapping rates obtained for as-irradiated iron as functions of irradiation temperature as derived from the data in Fig. 3 are shown in Fig. 4.

The annealing behaviour of the Fe specimens that were irradiated at 50°C is shown in Fig. 5. The lifetimes and intensities as functions of annealing temperature are shown by the filled symbols (in red). The iron specimens irradiated at 100°C have also been annealed. These results were published previously [12]. For comparison with the present data the annealing behaviour from [12] is shown by the line (in blue) in Fig. 5.

The trapping rates derived from the data in Fig. 5 are shown in Fig. 6.

Analysis of the lifetime spectrum for un-irradiated F82H (Fig. 2) shows that a population of defects is present already before irradiation and that they trap a major fraction of the positrons with a characteristic lifetime of 154 ps. The defects that trap positrons in the un-irradiated steel specimens may also be present in the irradiated specimens or they may have changed structure due to the irradiation or have interacted with other, irradiation produced, defects. The positron lifetime for these inherent defects is therefore uncertain. Furthermore this component probably merges with the shortlived component due to positrons annihilating in the bulk, resulting in the lifetime τ_1 (Fig. 3). One consequence of this mixing of short lifetimes is that it is very difficult to make realistic estimates of trapping rates and therefore also of the densities of voids and other defects in F82H steel based on the PAS results alone.

Electrical conductivity was measured for iron irradiated to doses in the range of 0.008 to 0.38 dpa at 50°C and at 100°C. In addition, the specimens irradiated at 50°C were annealed at 300°C for 50 hours to simulate a bake-out treatment [15]. The results of the measurements are shown in Fig. 7. They agree with conductivity data obtained in a wider dose range [16] and with results of annealing of iron irradiated at 100°C to a dose of 0.23 dpa [12].

A clear difference is observed in the conductivities for irradiations at 50°C and at 100°C. Irradiation at 50°C gives rise to a stronger decrease in conductivity than irradiation at 100°C.

5 Discussion

Generally, the quantitative results of the PAS measurements (Fig. 3) confirm the qualitative picture displayed in Figs. 1 and 2, viz. that for low temperature irradiation both Fe and F82H contain a population of voids as well as micro-voids. Details of the results, obtained both as function of irradiation temperature and for iron as function of annealing temperature will be discussed in the following.

5.1 As-irradiated Fe and F82H

In the as-irradiated state at the lowest irradiation temperatures ($T \leq 100^\circ\text{C}$) the two dominating lifetime components for both Fe and F82H are the two long-lived ones, with the lifetime values of $\tau_2 \sim 300 - 325$ ps and $\tau_3 \approx 500$ ps (Fig. 3). Both of these components must be ascribed to three-dimensional vacancy agglomerates, i.e. voids, but of different sizes. The shorter lifetime, $\tau_2 \sim 300 - 325$ ps, is equiva-

lent to average cavity sizes of $\sim 7 - 9$ vacancies [14], i.e. micro-voids. The longer lifetime of ~ 500 ps must be associated with voids that contain (on average) $\sim 40 - 50$ vacancies or more, as mentioned above. Although we ascribe the two lifetimes to two specific average void sizes, in reality they are likely to represent a two-bin approximation of one wide size distribution of voids rather than two discrete distributions of void sizes [16].

For iron, the trapping rate, κ_2 , for the micro-voids is estimated to be $\geq \sim 80 \text{ ns}^{-1}$ at 50°C and 100°C (Fig. 4). Taking the specific trapping rate for a void size of ~ 8 vacancies from [1], we obtain from Eq. (1) the density of micro-voids (C_{m-v}) to be $> \sim 1 \times 10^{24} \text{ m}^{-3}$. The trapping rate into the larger voids, κ_3 , is found to be $\geq 25 \text{ ns}^{-1}$ and $\geq 15 \text{ ns}^{-1}$ at 50°C and 100°C , respectively (Fig. 4). Assuming that the voids contain (on average) about 50 vacancies ($\sim 1 \text{ nm}$ in diameter) a void density (C_v) greater than $\sim 10^{23} \text{ m}^{-3}$ is obtained from Eq. (1). If the voids are bigger than assumed here, an estimate of their density will result in a lower value. The estimated total density of micro-voids and voids is in agreement with the density observed by TEM for a somewhat higher dose (0.7 dpa) [16].

When the irradiation temperature is increased to 200°C (Fe) and 250°C (F82H), τ_2 decreases strongly to about 200 ps for both materials (Fig. 3). This indicates that the micro-voids are not formed at these temperatures. The defects that give rise to the lifetime of $\sim 200 \text{ ps}$ could be very small, gas or impurity stabilised, vacancy clusters containing only a few vacancies. It cannot be excluded that these defects have also been present below 200°C , but that it has not been possible to resolve them in the lifetime spectra. This is because of the dominance of the micro-voids, which act as much stronger trapping centres for positrons than the small vacancy clusters, as can be seen by comparing κ_2 at 100°C and at 200°C (Fig. 4).

For iron irradiated at 200°C and 350°C , the trapping rate into the larger voids, κ_3 , is ≥ 6 and 1.5 ns^{-1} , respectively (Fig. 4). If the voids contain about 50 vacancies as assumed above, void densities of $C_v > \sim 4 \times 10^{22} \text{ m}^{-3}$ and $1 \times 10^{22} \text{ m}^{-3}$ are obtained (Eq. 1) for the irradiation temperatures of 200°C and 350°C , respectively. If the voids on average contain more than the assumed 50 vacancies, the estimated densities would be lower.

It is interesting to note here that the temperature dependence of the void density for iron determined by PAS is very similar to the one reported for voids observed by TEM in molybdenum neutron irradiated at the same homologous temperatures [17, 18].

The striking observation for the F82H steel is that after irradiation at 50°C voids and micro-voids are found to be present, for irradiation at 250°C apparently no voids are formed ($I_3 \approx 0\%$, Fig. 3), while irradiation at 350°C again leads to the formation of a population of voids ($I_3 \approx 5\%$). These observations seem to suggest that sinks for vacancies are present in the temperature range around 250°C that prevents a supersaturation of vacancies to build up, which would be necessary for void formation, and that at 350°C the sinks would be less efficient. Further investigations are necessary to clarify this.

It should be mentioned that no cavities can be observed by TEM in F82H neutron irradiated at 250°C to doses of 0.7 and 2.5 dpa [19], in agreement with our PAS results. Similarly, irradiation to 10 dpa at 310°C did not result in cavities visible by TEM [19].

5.2 Annealing of Fe

Figure 5 shows that the annealing behaviour of the PAS parameters for the iron specimens irradiated at 50°C and at 100°C is very similar. As a consequence, also the variation of the trapping rates with annealing temperature is very similar (Fig. 6 and [12]). The changes of the PAS parameters in different temperature ranges reflect the recovery of the microstructure during annealing. This has been discussed in some detail in [12]. The main observations are the following.

In the annealing temperature range of 50°C to about 250°C, κ_3 first increases and then flattens off (Fig. 6) which suggests that the density and/or the size of the voids increases and then stays constant. Simultaneously, κ_2 and therefore the micro-void density C_{m-v} decreases drastically while the increase of τ_2 (up to 250°C, Fig. 5) indicates an increase in the average micro-void size from less than 10 to 15 vacancies. Thus, the number density of voids increases at the expense of the micro-voids. This strong coarsening of the micro-void population takes place at temperatures well below the recovery stage V (250°C - 280°C [20]) the centre of which is indicated by a grey band in Figs. 3 - 6. Since stage V indicates the lower temperature at which vacancies can evaporate from micro-voids or voids, the decrease in density of the micro-voids below stage V must happen by their migration and coalescence with other micro-voids and voids [21, 22].

When the annealing temperature increases above stage V, τ_2 drops abruptly (Fig. 5). This indicates that the micro-void component disappears in this temperature range, which is also indicated by the steep decrease of κ_2 that extrapolates to zero at about Stage V (Fig. 6). Above Stage V, $\tau_2 \approx 200$ ps, which is a lifetime that could be due to very small, gas or impurity stabilised, vacancy clusters containing only a few vacancies, as mentioned earlier. Their density may be estimated to be $\sim 5 \times 10^{23} \text{ m}^{-3}$ [12] up to about 350°C. Above 350°C the density decreases to the detection limit at $\sim 500^\circ\text{C}$.

In the temperature range 250°C - 350°C, i.e. in and above the annealing stage V, the trapping rate for voids κ_3 decreases by a factor of more than ten (Fig. 6) and continues to decrease at the higher temperatures. This demonstrates clearly that in stage V the void density decreases, probably by coarsening of the void population due to Ostwald ripening.

An interesting result of the annealing of the irradiated iron is that there is no significant difference in the PAS results for the as-irradiated or annealed specimens for irradiation at 50°C and at 100°C (Fig. 5). This is contrary to the electrical conductivity results, which show a clear difference between the data at 50°C and at 100°C (Fig. 7). As discussed below, we associate the conductivity differences to the behaviour of carbon at the two irradiation temperatures. Detailed PAS measurements have clearly shown the binding of carbon to vacancies and vacancy clusters and the influence of carbon on the annealing behaviour of irradiated iron for carbon concentrations of the same order of magnitude as the vacancies and vacancy clusters [23, 24]. Hence, we conclude that the close similarity of the annealing behaviour of iron irradiated at 50°C and at 100°C is due to a low concentration of carbon, in agreement with the low nominal carbon level in the specimens (Table 1).

5.3 Electrical Conductivity

The results for the electrical conductivity as function of dose in Fig. 7 show three major effects. The first one is the general trend at both irradiation temperatures (50°C and 100°C) of a decrease in conductivity with increasing dose. This is in agreement with measurements for iron in a wider dose range [16] and with the dose dependence observed for copper irradiated at 100°C [15]. The decrease has been ascribed to the increasing density of radiation created defects and their clusters and to a smaller extent to transmutation created impurities [12].

The second effect is that the conductivity observed after irradiation at 50°C is lower compared to the conductivity after irradiation at 100°C. We suggest that this difference may be associated with the fact that carbon is immobile at 50°C, but migrates above $\sim 70^\circ\text{C}$ [23, 24]. Thus at 100°C precipitation of carbon may take place to sinks such as dislocations [25]. This will reduce the average scattering of electrons and therefore increase the electrical conductivity compared to the situation at 50°C when the carbon atom impurities are trapped in interstitial positions.

The third effect to note is the increase in electrical conductivity with dose after annealing at 300°C. This effect may be a result of irradiation enhanced diffusion of impurities that leads to an increasing precipitation of impurities with dose. As mentioned above, the reduction of the conductivity with dose in the as-irradiated state is considered to be mainly due to the irradiation created defects. Recovery of a major part of the defect structure on annealing at 300°C leaves as electron scattering centres mainly the impurities and their precipitates, the effect of which on the conductivity will be smallest at the highest doses.

6 Summary

The present work demonstrates that positron annihilation spectroscopy (PAS) can provide valuable information about the microstructure of irradiated metals, in particular about the behaviour of voids and sub-microscopic voids (micro-voids).

The results demonstrate that the formation of voids takes place during neutron irradiation of pure iron at temperatures in the range of 50°C - 350°C. For irradiation temperatures of 50°C and 100°C also a high density of micro-voids was observed. The densities of the voids are the same as found in molybdenum, neutron irradiated at the same homologous temperatures to about the same dose.

Voids and micro-voids were also detected in low activation F82H steel for a low irradiation temperature (50°C), while for irradiation close to the temperature of annealing stage V (250°C) no voids or micro-voids could be detected. Surprisingly, irradiation at the higher temperature of 350°C again resulted in void formation. Further investigations of this phenomenon are planned.

The annealing behaviour of iron irradiated at 50°C and at 100°C does not show any significant difference. Coarsening of the micro-void and void population takes place below stage V by migration and coalescence of the micro-voids and voids.

Measurements of the dose dependence of the electrical conductivity of iron irradiated at 50°C and at 100°C shows a lower conductivity for the specimens irradiated

at 50°C. This is associated with segregation of carbon at about 70°C where carbon becomes mobile.

Acknowledgement

The present work was partly funded by the European Fusion Technology Programme. We wish to thank B. Olsen and N. J. Pedersen for technical assistance.

References

- [1] M. Eldrup and B.N. Singh, J. Nucl. Mater. 251 (1997) 132.
- [2] M. Eldrup, J. Phys. (Paris) IV Colloq. 5 (1995) C1-93.
- [3] M. Eldrup, J.H. Evans, O.E. Mogensen, and B.N. Singh, Rad. Effects 54 (1981) 65.
- [4] Y. Kamimura, T. Tsutsumi and E. Kuramoto, Phys. Rev. B 52 (1995) 879.
- [5] E. Kuramoto, H. Abe, M. Takenaka, F. Hori, Y. Kamimura, M. Kimura, K. Ueno, J. Nucl. Mater. 239 (1996) 54.
- [6] K. Ueno, M. Ohmura, M. Kimura, Y. Kamimura, M. Takenaka, T. Tsutsumi, K. Ohsawa, H. Abe and E. Kuramoto, Mat. Sci. Forum 255-257 (1997) 430.
- [7] K.O. Jensen and R.M. Nieminen, Phys. Rev. B 36 (1987) 8219.
- [8] M. Puska and R.M. Nieminen, J. Phys. F: Metal Physics 13 (1983) 333.
- [9] M. Eldrup, Mat. Sci. Forum 105-110 (1992) 229.
- [10] H. Häkkinen, S. Mäkinen and M. Manninen, Phys. Rev. B 41 (1990) 12441.
- [11] B.N. Singh, D.J. Edwards, M. Eldrup, P. Toft, Risø Report, Risø-R-937(EN), Jan. 1997.
- [12] M. Eldrup and B.N. Singh, J. Nucl. Mater. 276 (2000) 269.
- [13] P. Kirkegaard, N.J. Pedersen and M. Eldrup, Risø Report, Risø-M-2740, 1989.
- [14] M. Puska and R.M. Nieminen, Rev. Mod. Phys. 66 (1994) 841.
- [15] M. Eldrup and B.N. Singh, J. Nucl. Mater. 258 - 263 (1998) 1022.

- [16] M. Eldrup, B.N. Singh, S.J. Zinkle, T.S. Byun and K. Farrell, Proceedings of the 10th Int. Conf. on Fusion Reactor Materials, Baden-Baden, Oct. 2001 (to be published).
- [17] S.I. Golubov, B.N. Singh and H. Trinkaus, J. Nucl. Mater. 276 (2000) 78.
- [18] J. Bentley, B.L. Eyre and M.H. Loretto, in: M.T. Robinson and F.W. Young, Jr (Eds.), Fundamental Aspects of Radiation Damage in Metals (US-ERDA Conf.-751006), 1975, p. 925.
- [19] R. Schäublin and M. Victoria, J. Nucl. Mater. 283 - 287 (2000) 339.
- [20] H. Schultz, P. Ehrhart, in: Landolt-Börnstein, New Series, Vol. 25, Atomic Defects in Metals, H. Ullmaier (ed), Springer.
- [21] P.J. Goodhew and S.K. Tyler, Proc. R. Soc. A377 (1981) 151.
- [22] B.N. Singh and A.J.E. Foreman, in: R.S. Nelson (Ed.), Consultant Symposium; The Physics of Irradiation Produced Voids, AERE-R7934, H.M. Stationary Office, January 1975, p. 205; Scripta Met. 9 (1975) 1135.
- [23] A. Vehanen, P. Hautojärvi, J. Johansson, J. Yli-Kauppila and P. Moser, Phys. Rev. B25 (1982) 762.
- [24] P. Hautojärvi, L. Pöllänen, A. Vehanen, and J. Yli-Kauppila, J. Nucl. Mater. 114 (1983) 250.
- [25] T. Takeyama and H. Takahashi, in Fundamental Aspects of Radiation Damage in Metals, ed. M.T. Robinson and F.W. Young, Jr. (ERDA, Oak Ridge, 1976), p. 1100.

Table 1. Chemical composition of pure iron (in atomic ppm) and F82H (in weight %)

ELEMENTS	F82H (wt. %)	Pure Fe (ppm)
C	0.09	0.009
Si	0.11	15
Mn	0.16	3
S	0.002	2
P	0.002	3
Cr	7.70	8
Ni	0.02	2
Mo	0.003	7
V	0.16	0.07
Nb	0.002	0.4
Al	0.003	10
B	0.0002	3
N	0.007	-
Co	0.005	4
Cu	0.01	4

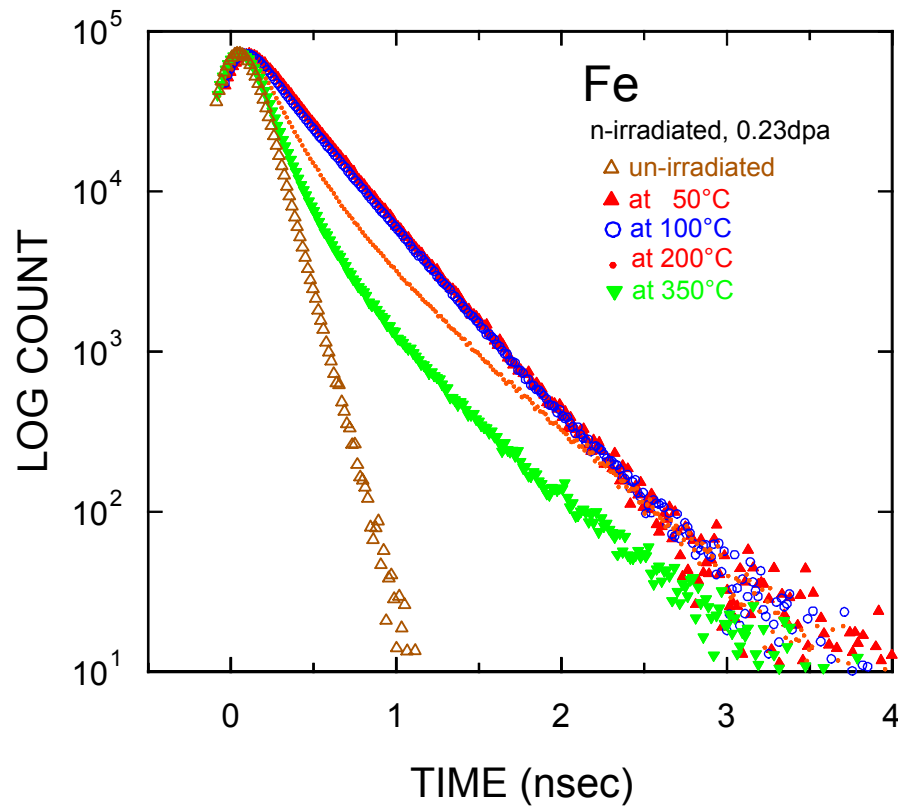


Fig. 1. Positron lifetime spectra for iron neutron irradiated to 0.23 dpa at different temperatures. The spectrum for un-irradiated iron is shown for comparison. The long lifetimes are indicative of the presence of micro-voids and voids.

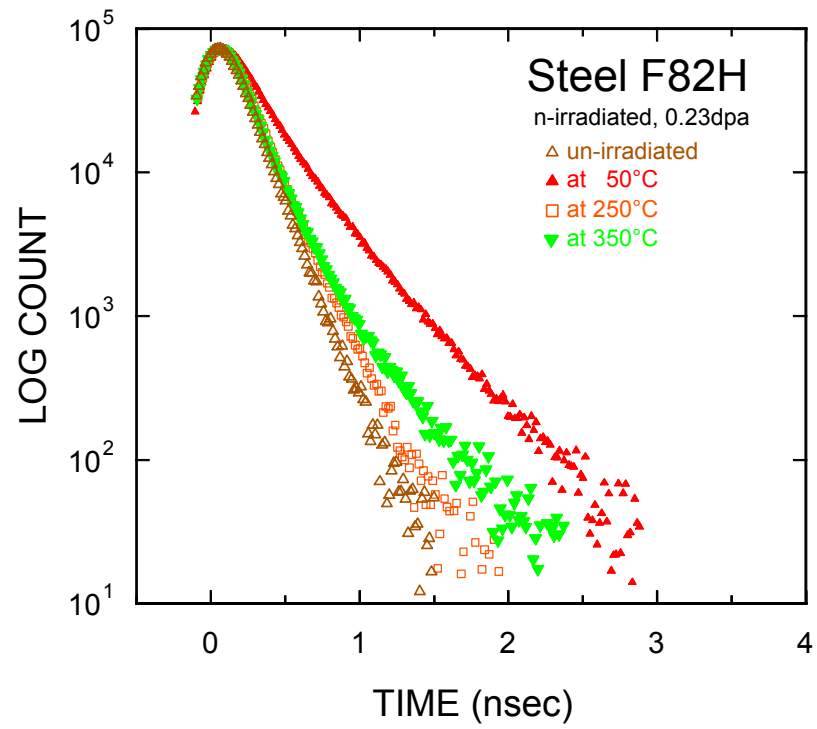


Fig. 2. Positron lifetime spectra for F82H steel neutron irradiated to 0.23 dpa at different temperatures. The spectrum for un-irradiated steel is shown for comparison. The longest lifetimes are indicative of the presence of micro-voids and voids.

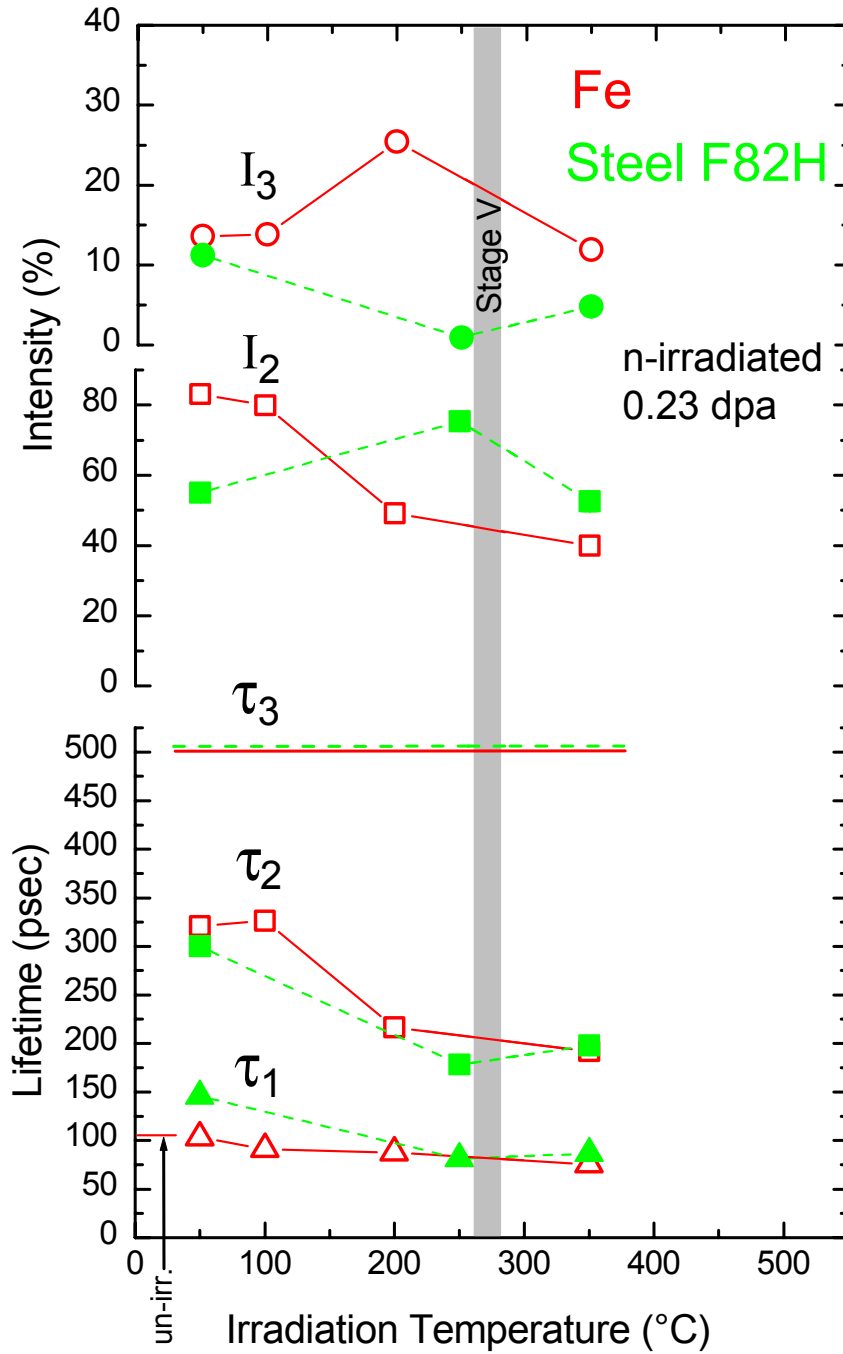


Fig. 3. The three positron lifetimes and the intensities of the two long-lived components ($I_1 + I_2 + I_3 = 100\%$) extracted from the spectra in Figs. 1 and 2 for the neutron irradiated Fe (open symbols connected with full lines) and F82H (closed symbols connected with dashed lines) as functions of irradiation temperature. The longest lifetime, τ_3 , was fixed at 500 ps in the spectrum analysis. The shaded band indicates the temperature of the recovery stage V.

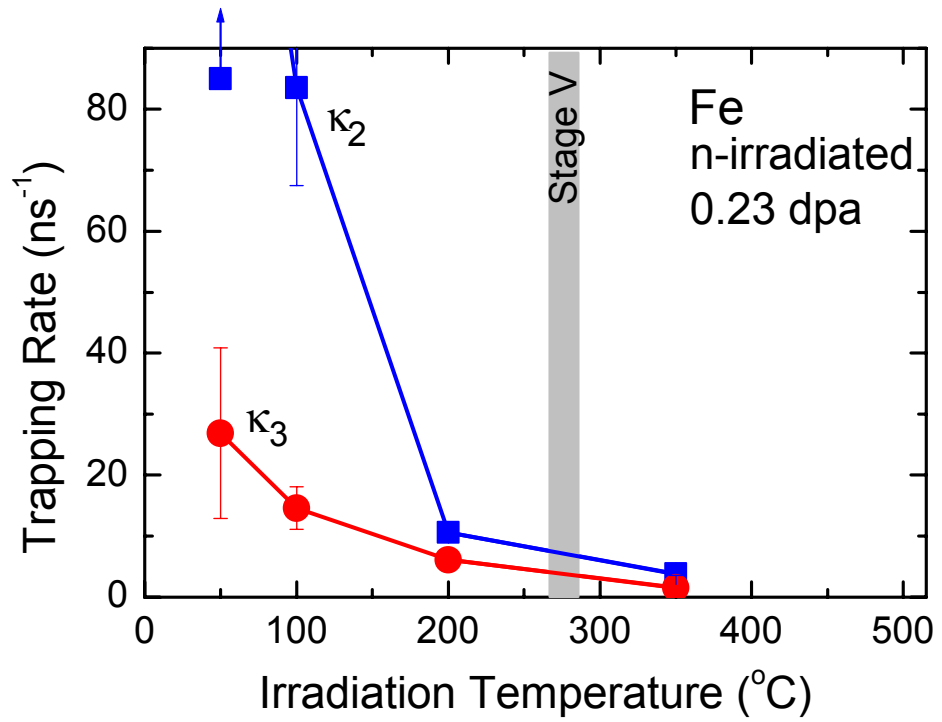


Fig. 4. The positron trapping rates into defects in the neutron irradiated Fe as functions of irradiation temperature, derived from the data in Fig. 3. The circles are for trapping into voids ($\tau_3 = 500$ ps) and the squares into micro-voids (at 50 and 100°C) or small clusters (at higher temperatures). The indicated error bars are based on the statistical scatter of the data points in the lifetime spectra. The shaded band indicates the temperature of the recovery stage V.

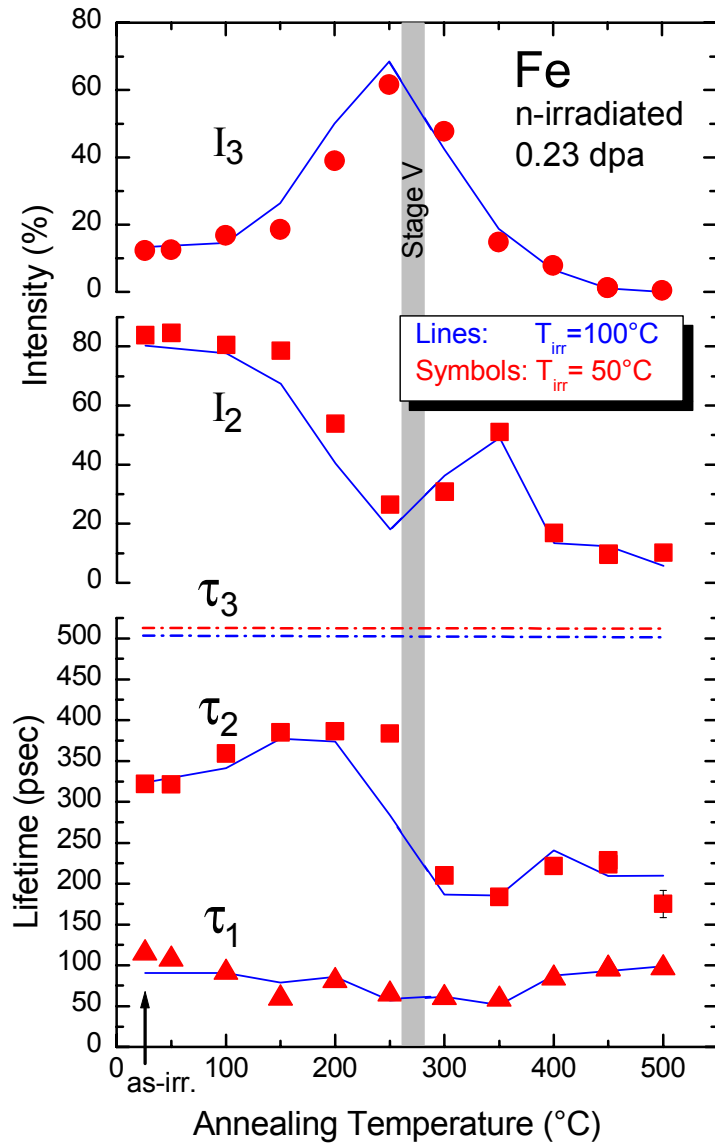


Fig. 5. The three positron lifetimes and the intensities of the two long-lived components ($I_1 + I_2 + I_3 = 100\%$) extracted from the spectra for the neutron irradiated Fe as functions of annealing temperature. The longest lifetime, τ_3 , was fixed at 510 ps in the spectrum analysis. The symbols are for iron irradiated at 50°C while the lines represent results for iron irradiated at 100°C [12]. The shaded band indicates the temperature of the recovery stage V.

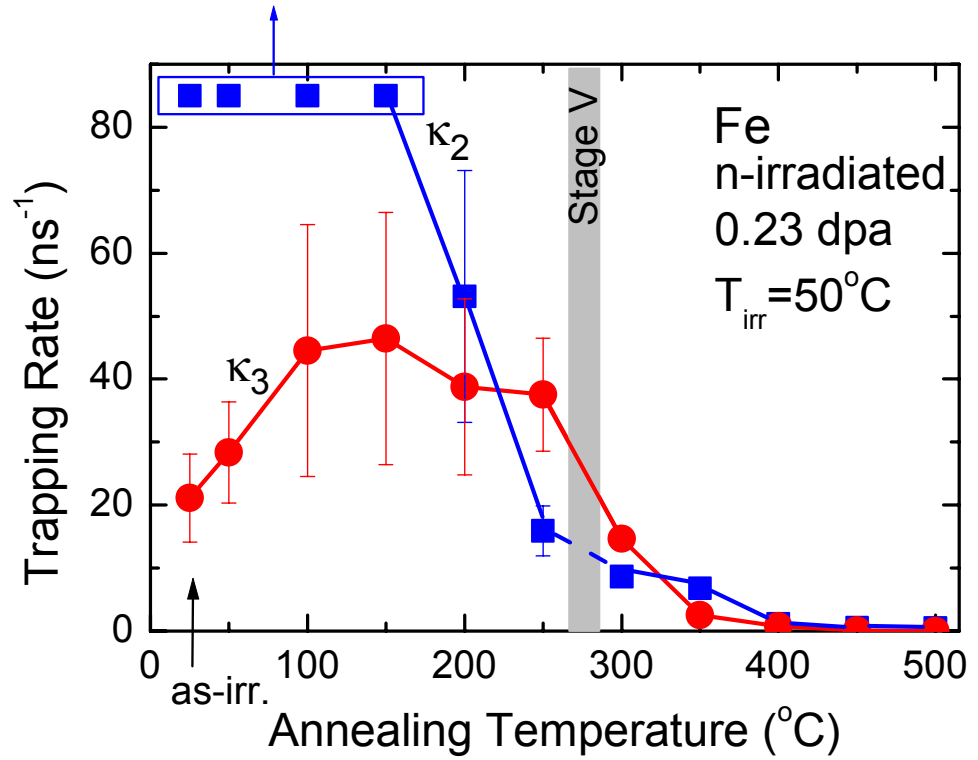


Fig. 6. The positron trapping rates into defects in the neutron irradiated Fe as functions of annealing temperature. The circles are for trapping into voids and the squares into micro-voids (for $T \leq 250^{\circ}\text{C}$) or small clusters (at higher temperatures). The indicated error bars are based on the statistical scatter of the data points in the lifetime spectra. For temperatures at and below 150°C the points for κ_2 are above the frame of the figure. The shaded band indicates the temperature of the recovery stage V.

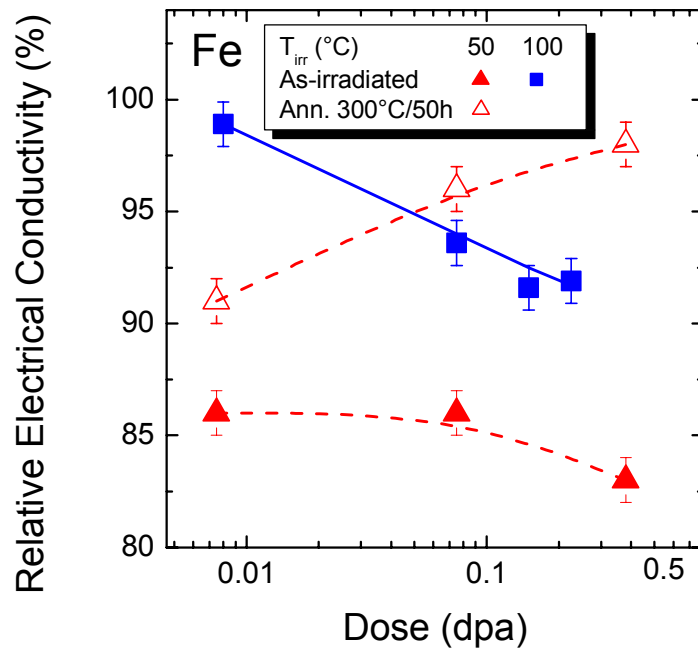


Fig. 7. Electrical conductivity as a function of radiation dose for Fe irradiated at 50°C and at 100°C. Results for the former specimen are shown for the as-irradiated state and after annealing at 300°C for 50 hours. The plot shows the conductivity relative to that for un-irradiated Fe.

Title and authors

Investigations of Void Formation in Neutron Irradiated Iron and F82H Steel

M. Eldrup and B.N. Singh

ISBN	ISSN
87-550-2824-1 87-550-2826-8(Internet)	0104-2840
Department or group	Date
Materials Research Department	December 2001
Groups own reg. number(s)	Project/contract No(s)

Sponsorship

Pages	Tables	Illustrations	References
21	1	7	25

Abstract (max. 2000 characters)

In the present work pure iron and low activation steel F82H have been neutron irradiated at temperatures in the interval 50°C - 350°C to a dose of 0.23 dpa (displacements per atom). The formation of defects has been investigated by the use of positron annihilation spectroscopy (PAS). In addition iron has been irradiated to different doses in the range 0.01 - 0.4 dpa at 50°C and 100°C and the dose dependence of the electrical conductivity determined.

The results demonstrated that the formation of voids takes place during neutron irradiation of pure iron in the whole temperature range. For irradiation temperatures of 50°C and 100°C also a high density of micro-voids was observed. Voids and micro-voids were also detected in low activation F82H steel for a low irradiation temperature (50°C), while for irradiation close to the temperature of annealing stage V (250°C), no voids or micro-voids could be detected. Surprisingly, irradiation at the higher temperature of 350°C again resulted in void formation. The annealing behaviour of iron irradiated at 50°C and at 100°C did not show any significant difference. Coarsening of the micro-void and void population takes place below stage V by migration and coalescence of the micro-voids and voids.

The dose dependence of the electrical conductivity of iron showed a lower conductivity for the specimens irradiated at 50°C than at 100°C. This has been associated with the segregation of carbon at about 70°C where carbon becomes mobile.

Descriptors INIS/EDB

ANNIHILATION; DEFECTS; ELECTRIC CONDUCTIVITY; FERRITIC STEELS; FISSION NEUTRONS; IRON; IRRADIATION; POSITRONS; SPECTROSCOPY; TEMPERATURE DEPENDENCE; VOIDS

Available on request from Information Service Department, Risø National Laboratory,
(Afdelingen for Informationsservice, Forskningscenter Risø), P.O.Box 49, DK-4000 Roskilde, Denmark.
Telephone +45 4677 4004, Telefax +45 4677 4013